Low power nonlinear effects in the ferromagnetic resonance of yttrium iron garnet

Kevin D. McKinstry, Carl E. Patton, and Milind Kogekar
Department of Physics, Colorado State University, Fort Collins, Colorado 80523

(Received 24 January 1984; accepted for publication 4 March 1985)

Ferromagnetic resonance (FMR) absorption was observed in a spherical single-crystal sample of $Y_3Fe_5O_{12}$ (YIG) at 9.5 GHz and room temperature. Resonance absorption curves were obtained as a function of microwave power level and duty cycle for different static field directions relative to the crystal axes. Foldover effects and other nonlinear behavior were seen at microwave field amplitudes (h_{rf}) between 9 and 50 mOe with the applied static field in the (110) plane. When FMR absorption is observed with a high power cw signal ($h_{rf} = 50$ mOe) with the biasing field along either the [100] or the [110] directions and decreasing in magnitude, an absorption curve is obtained that has a long broad shoulder which is shifted below the low power FMR biasing field position. With increasing field in these directions, the absorption curve develops a cusp below the low power biasing field position. With the bias field in the [111] direction the absorption curve shows cusps for both increasing and decreasing fields at this power level. Field shifts in the observed resonance spectra do not converge to the zero anisotropy resonance field value, but to a field value below the low power [110] direction FMR field position. These effects disappear when the experiments are carried out using pulsed microwaves with a pulse width of 100 μsec and duty cycles below 1%. These phenomena are therefore attributed to the effects of heating on the magnetocrystalline anisotropy properties of single-crystal YIG. The quantitative results, however, are not in accord with simple heating considerations.

INTRODUCTION

The ferromagnetic resonance (FMR) in yttrium iron garnet, $Y_3Fe_5O_{12}$, often referred to as YIG, is of considerable interest because of the material's narrow resonance line width and the resulting nonlinear microwave behavior at moderate power levels. Such nonlinear effects can give the FMR absorption a peculiar distortion which depends on the direction of sweep for the applied field, much like the curves in Figs. 3–9 of this paper. These distortions have been given the label "foldover."[1,2] Various workers have investigated the physical origins of foldover in FMR. Weiss[1] reported low power nonlinear effects in YIG disks and later presented an explanation based on spin temperature.[2] The effect on resonance due to crystalline anisotropy was examined by Gottlieb.[3] He showed that, to lowest order, the shift in resonance frequency is proportional to the square of the FMR precession cone angle and that this quadratic term could lead to foldover. Masters,[4] employing a continuous wave rf source, observed shifts of the resonance field with power in single-crystal YIG spheres and determined that these shifts were due entirely to heating effects at resonance and the resulting drop in the magnetocrystalline anisotropy field.

This paper presents experimental results which extend the work of Masters. The sample for the resonance experiments was an oriented single-crystal YIG sphere. FMR absorption versus field profiles were obtained as a function of cw microwave field amplitude, applied field sweep rate, and crystal orientation with respect to the field. Further data were also obtained with pulsed microwaves for different duty cycles. The observed foldover effects in some cases were quite dramatic. With increasing power level, large shifts and distortions of the narrow FMR absorption peak were observed, with the direction of the shift dependent on the orientation of the crystal. Field sweeps in the opposite direction (for a given orientation) yielded sharp cusplike absorption profiles. All spectra were very sensitive to sweep rate. Foldover effects disappeared when the sample was excited with pulsed microwaves at a low duty cycle. While similar to the results of Masters,[4] the positions of the cusps and shoulders of the high power absorption curves are not completely consistent with a mechanism based on simple heating considerations as proposed in Ref. 4.

EXPERIMENT

Ferromagnetic resonance absorption curves were obtained at room temperature and a microwave frequency of 9.5 GHz using a modified Varian EPR spectrometer. The instrumentation is shown schematically in Fig. 1. The sample was mounted in the center of the *x*-band waveguide short one-half wavelength from the shorting plate. The reflected microwave power was monitored with a conventional diode detector. The precision attenuator on the klystron side of the circulator was used to control power incident on the sample. The second precision attenuator in the detector arm was used in a complimentary manner so that all data could be obtained with approximately the same power at the detector. The *pin* diode modulator was used to obtain pulsed microwave power at the sample with pulse lengths from 5 μsec to 10 msec and a duty cycle from 1 to 75%. The klystron was stabilized on the cavity dip of the cavity wavemeter, set to 9.5 GHz $\pm$ 1 MHz by means of a direct reading microwave counter in the detector arm which was accurate to better than 1 kHz. The peak power at 9.5 GHz was 258 mW, corresponding to a microwave field amplitude of 50 mOe at the sample. For each FMR absorption profile in Figs. 3–9 the

 0021-8979/85/140925-05$02.40 © 1985 American Institute of Physics

Downloaded 26 Dec 2001 to 129.82.140.114. Redistribution subject to AIP license or copyright, see http://ojps.aip.org/japo/japcr.jsp

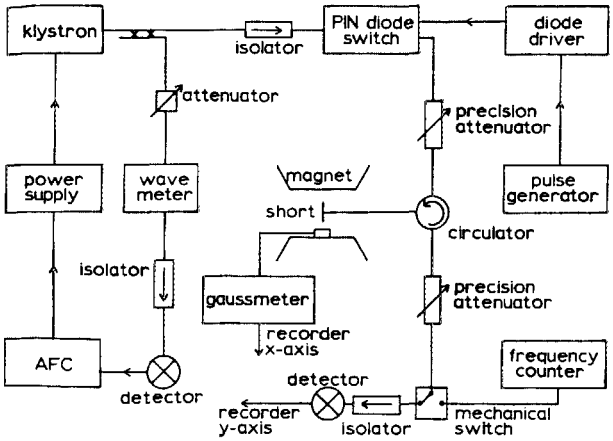

FIG. 1. Schematic diagram of the experimental apparatus used to record the ferromagnetic resonance absorption curves.

applicable microwave field amplitude is indicated in mOe.

The sample was a polished single-crystal YIG sphere 1.339-mm diameter with an absorption linewidth of 3.2 Oe, somewhat larger than the 0.5-Oe value expected for highly polished, impurity-free single-crystal YIG. It was aligned using x-ray precession camera methods and mounted on a turntable for rotations in the (110) plane of the crystal. The microwave and dc magnetic fields were mutually perpendicular and both in the (110) plane of the crystal. An NMR gaussmeter was used to calibrate the static magnetic field, which was then measured with an accuracy of $\pm$ 1 Oe.

FMR spectra were obtained by sweeping the magnetic field at a fixed rate and monitoring the reflected power versus field. To confirm proper alignment of the sample, spectra were obtained for various angles between the magnetic field and the [100] direction. The incident microwave power was kept below the level necessary for distortion of the low power absorption curve. Values of the magnetic field for resonance with the bias along the [100] and [$\bar{1}$00] directions were within 1 Oe of each other, indicating proper alignment to within the accuracy of the experiment. The resonance field H_0 versus crystal orientation is shown in Fig. 2. The solid points represent measured values. The solid line was generated from Eq. (1) in the discussion section, with $K_1/M_0 = -39$ Oe. The dotted line in the figure indicates the theoretical FMR location in the absence of magnetocrystalline anisotropy. This "zero anisotropy FMR position" will be important in the discussion to follow.

Figures 3–5 show the effect of increasing microwave field amplitude (and power) on the FMR absorption profile for a static applied field along the three principal crystallographic directions. Arrows on the absorption curves denote directions of sweep; the sweep rate in each case was 50 Oe/min. The small field shift between the upsweep and downsweep curves seen at lower powers has been attributed to instrumentation.

In Fig. 3 the magnetic field is along the [100] direction. Asymmetries in the absorption curve first appear at a microwave field amplitude of 3 mOe, and foldover effects become evident at 9 mOe. As the microwave power is increased further, the upsweep curve develops into a sharp cusp slightly below the low power resonance position. The downsweep curve becomes extremely distorted as the power is increased and evolves into an abrupt shoulder far below the low power FMR position. At maximum power a small discontinuity is observed in the downsweep curve just above the shoulder.

The FMR curves versus microwave field amplitude with the magnetic field along the [111] direction are shown in Fig. 4. Changes in the absorption which result from increasing the incident microwave power in this case are not nearly as dramatic as those for the [100] direction. The resonance field shifts and distortions that do occur, however, are in the opposite direction. As the incident power is increased,

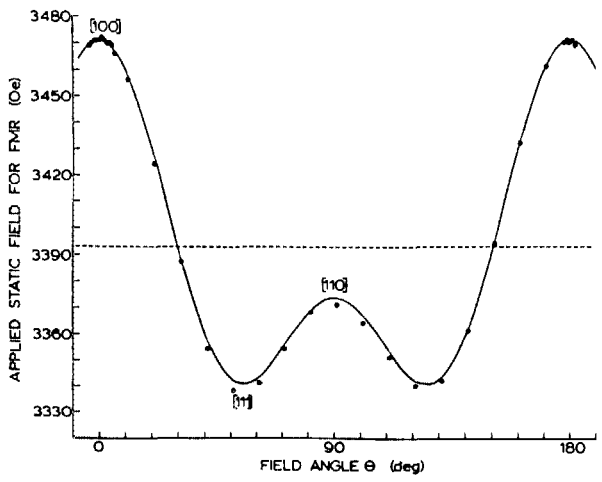

FIG. 2. Low power ferromagnetic resonance field vs field (and magnetization) angle for rotations in the (110) plane. The [100] direction is taken as 0°. Data were obtained using a YIG sphere at room temperature with a microwave frequency of 9.5 GHz and microwave field amplitude of 2 mOe (0.3 mW).

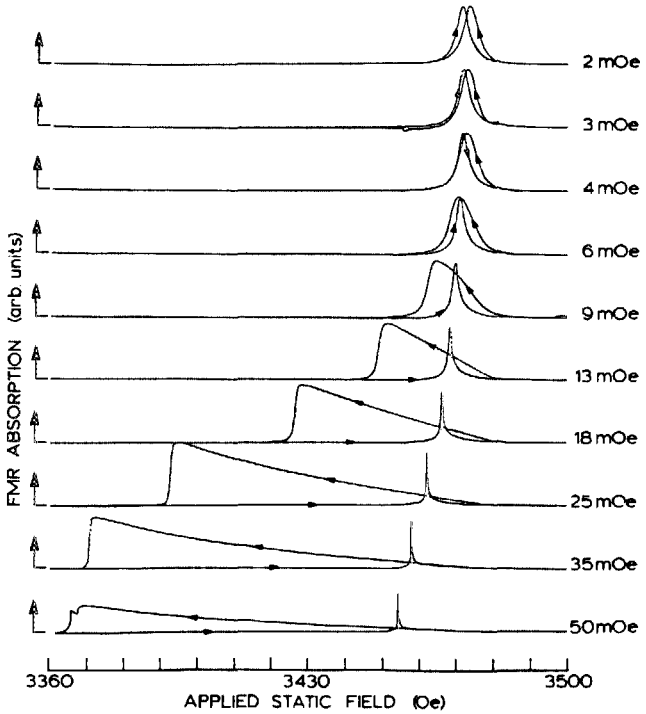

FIG. 3. Upsweep and downsweep ferromagnetic resonance absorption curves vs incident power for the single-crystal sphere of YIG at room temperature and 9.5 GHz. The applied field is in the [100] direction and swept at 50 Oe/min. The incident microwave field amplitude corresponding to each set of curves is indicated in mOe. Arrows denote directions of sweep.

Downloaded 26 Dec 2001 to 129.82.140.114. Redistribution subject to AIP license or copyright, see http://ojps.aip.org/japo/japcr.jsp

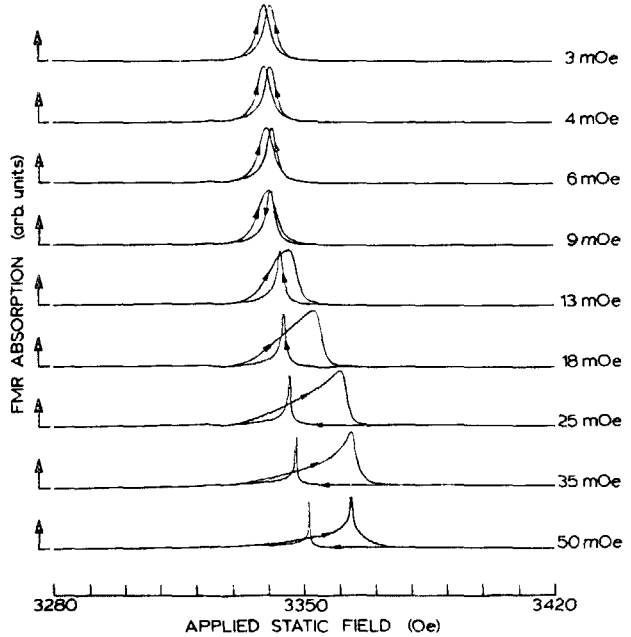

FIG. 4. Upsweep and downsweep FMR absorption curves as in Fig. 3 but with the applied static field in the [111] direction.

small asymmetries in the FMR curves are obtained at 6 mOe, and foldover is apparent at 13 mOe. The upsweep curve evolves into a cusp about 20 Oe above the low power FMR position. The downsweep curve, on the other hand, broadens to a distinct shoulder at 18 mOe and then also develops a cusp at maximum power.

Figure 5 shows the set of FMR absorption curves for the dc magnetic field in the [110] direction. High power effects in this case are even smaller than those for [111]; asymmetries in the curves do not occur until the microwave field amplitude is 9 mOe, and foldover is not evident until 35 mOe. At maximum power the upsweep curve has evolved to a cusp slightly above the low power FMR field position. The downsweep curve broadens to a complicated absorption with a peak somewhat above the low power FMR position, followed by a decorated shoulder below the low power position. The shoulder apparent in the downsweep curve at maximum power in Fig. 5 is virtually identical to the corresponding profile in Fig. 3 and occurs at the same field value as well.

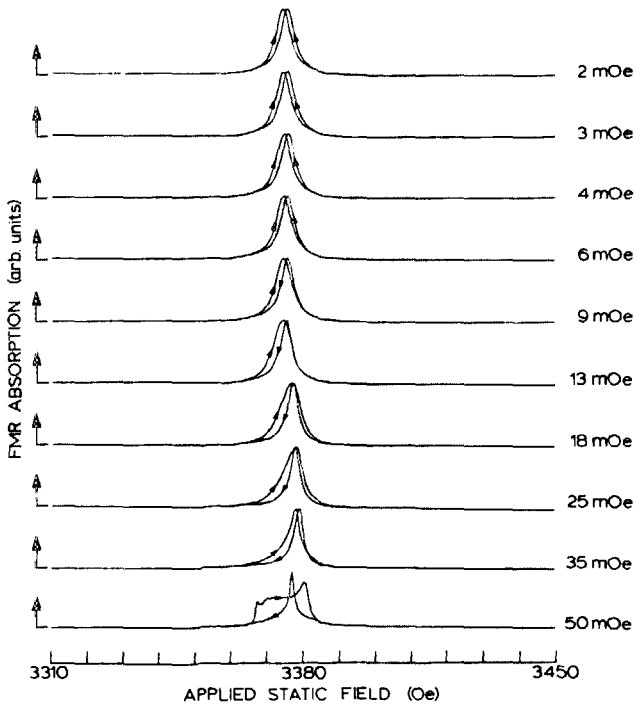

FIG. 5. Upsweep and downsweep FMR absorption curves as in Fig. 4 but with the applied field in the [110] direction.

The nonlinear effects shown in Figs. 3–5 were found to be strongly dependent on the static field sweep rate. A typical example of this effect on the resonance spectra is shown in Fig. 6, where the applied static field is in the [100] direction and the incident microwave field amplitude is 25 mOe. The upsweep curve forms a sharper and steeper cusp, and it occurs at successively lower field values as the sweep rate is decreased. The downsweep curve behaves in a similar manner, becoming a sharper and more abrupt shoulder at lower sweep rates. Field positions for the cusp and shoulder features of the upsweep and downsweep curves appear to be approaching limiting values at very slow sweep rates.

Limiting forms of the FMR spectra at maximum power and minimum sweep rate were obtained with the field in the three principal directions. These results are compared in Fig. 7, where resonance absorption curves for the [100], [111], and [110] directions at maximum incident microwave power (258 mW, 50 mOe) and minimum sweep rate (2.5 Oe/min) are shown. Under these experimental conditions resonance tails for the upsweep and downsweep curves coincide almost exactly. Experimental low power resonance field values for the three orientations are indicated by the pointer below each curve. The FMR field position at 9.5 GHz in the limit of zero magnetocrystalline anisotropy ($H_{\omega/\gamma}$) is indicated by the dotted line. This information will be pertinent to the discussion in the next section. This figure illustrates several trends and certain unusual features. For [100] and [111] the shifts are from the low power FMR position toward $H_{\omega/\gamma}$, down to approximately 3370 Oe. For [111] the shift is to higher fields, but only to about the same range. For [110] the cusp lies close to the low power FMR position while the shoulder profile straddles this position.

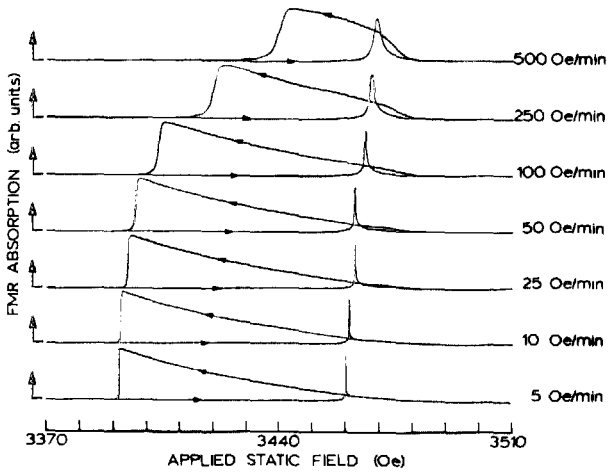

FIG. 6. Upsweep and downsweep FMR absorption curves as in Fig. 5 but as a function of sweep rate. The applied field is in the [100] direction, and the incident microwave field amplitude is 25 mOe.

Downloaded 26 Dec 2001 to 129.82.140.114. Redistribution subject to AIP license or copyright, see http://ojps.aip.org/japo/japcr.jsp

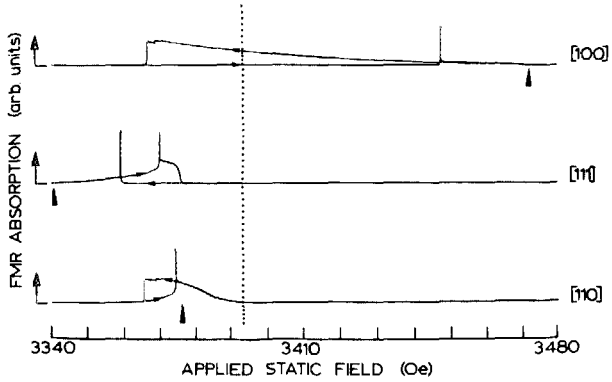

FIG. 7. Upsweep and downsweep FMR absorption curves for the [100], [111], and [110] directions at 9.5 GHz. The incident microwave field amplitude is 50 mOe, and the sweep rate is 2.5 Oe/min. Low power (2-mOe incident microwave field amplitude) FMR positions are indicated by pointers below the field axes. The FMR position in the limit of zero magnetocrystalline anisotropy, $H_{\omega/\gamma}$, is indicated by a broken line.

In Ref. 4 an explanation for the observed resonance curve shifts and distortions based on sample heating was presented. To investigate the effects of sample heating by the microwave driving field, absorption curves were produced using different pulse lengths and duty cycles to reduce the average power incident on the sample. For a given sweep rate and peak power, the shifts and distortions were found to be unchanged for pulse lengths spanning the available range of 5 μsec to 10 msec. Figure 8 shows an example of these results for a pulse length of 100 μsec. The static field is along the [100] direction and swept at 50 Oe/min. The peak microwave field amplitude is 17 mOe; duty cycles ranging from 1 to 100% were used. As the duty cycle is increased, the curves evolve substantially, the same as those in Fig. 3, showing similar cusp and shoulder features in the upsweep and

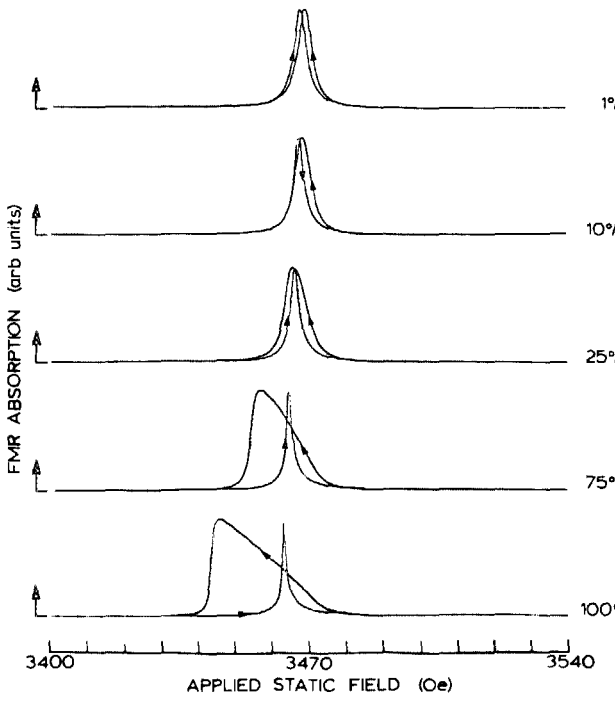

FIG. 8. Upsweep and downsweep FMR absorption curves as in Fig. 7 but as a function of average power incident on the sample. The applied field is in the [100] direction, and the peak incident microwave field amplitude is 17 mOe.

downsweep curves. The 100% duty cycle curves show a good correspondence to the 13- and 18-mOe curves in Fig. 3. A comparison of the low power profiles in Fig. 3 with the 0.1% duty cycle profiles in this figure indicates that an excessive duty cycle accounts for almost all of the foldover effects reported herein. However, as will be evident from the discussion to follow, the quantitative results are not consistent with the simple idea of a decrease in the anisotropy field due to heating.

DISCUSSION

The high-field FMR resonance condition for a YIG sphere with the static field in the (110) plane and the sample magnetization fully aligned in the field direction may be approximated by[5]

$$\omega/\gamma = H_0 + K_1/M_0(2 + 15/2 \sin^4\theta - 10 \sin^2\theta), \quad (1)$$

where ω is the resonance frequency, γ is the applicable gyromagnetic ratio, H_0 is the applied dc magnetic field, K_1 is the first-order magnetocrystalline anisotropy constant, M_0 is the saturation magnetization, and θ is the angle $\mathbf{M}_0$ and $\mathbf{H}_0$ make with the [100] crystallographic direction with both $\mathbf{M}_0$ and $\mathbf{H}_0$ in the (110) plane. It is assumed that H_0 is sufficiently large so that $\mathbf{M}_0$ and $\mathbf{H}_0$ are essentially parallel. A curve fit (Fig. 2) of the experimental values using Eq. (1) gives $K_1/M_0 = -39$ Oe, which is in reasonable agreement with the literature values of -40 to -45 Oe.[6]

Several theories have been formulated to explain certain nonlinear components of the absorption curve. The theory of parametric spin-wave excitation leading to nonlinear behavior at high power levels[7] has been used extensively. The second-order nonlinear threshold field amplitude at FMR for linearly polarized microwaves is given by

$$h_{\text{crit}} = \Delta H(\Delta H_k/4\pi M_s)^{1/2}, \quad (2)$$

where ΔH is the FMR linewidth and ΔH_k is the spin-wave relaxation rate expressed in linewidth units. For $\Delta H = 3$ Oe and $\Delta H_k = 0.5$–1.0 Oe, h_{crit} is on the order of 50 mOe or more, well above the 4–10 mOe thresholds in the data presented above. These comparisons, along with the absence of transient effects, would appear to rule out spin-wave instability as a cause of the present results.

An explanation for the basic shape of the high power absorption curves was presented in Ref.8. The basic idea is that the ordinary FMR field position can become "mobile" under heating and the consequent decrease in $|K_1|/M_0$. The FMR field position will therefore move toward $H_{\omega/\gamma}$ as the applied field moves up the tail of the FMR absorption from either side. If the field is also approaching $H_{\omega/\gamma}$ as it is approaching the FMR peak, the resonance position "runs away" from the approaching field, and one would expect the apparent absorption profile to assume the broad peak–abrupt shoulder shape presented in earlier figures. If the field is moving away from $H_{\omega/\gamma}$ as it approaches the FMR peak, the heating (and corresponding decrease in $|K_1|/M_0$) would cause the FMR position to move toward and through the approaching field. This profile would have a sharp cusp at the point of crossing.

This explanation seems satisfactory for the basic shapes of the upsweep and downsweep curves for the [100] and

Downloaded 26 Dec 2001 to 129.82.140.114. Redistribution subject to AIP license or copyright, see http://ojps.aip.org/japo/japcr.jsp

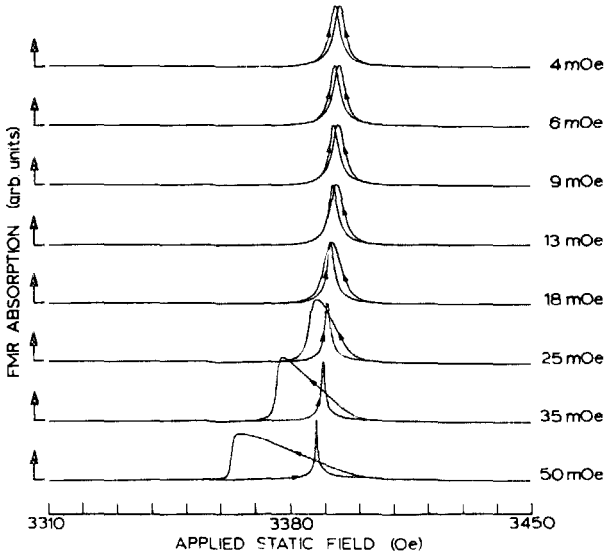

FIG. 9. Upsweep and downsweep FMR absorption curves as in Fig. 5 but for an orientation angle θ of $\sim 30°$, corresponding to a low power FMR field which should be independent of K_1/M_0 and equal to $H_{\omega/\gamma}$ as discussed in text.

[110] data, and qualitatively accounts for the sweep rate dependence of the absorption curves shown in Fig. 6. Beyond this, however, a simple heating model appears unsatisfactory. The primary problem is in the shoulder positions for the profiles obtained for maximum power and slowest sweep rate. According to the model, heating would cause all shoulders to approach the $H_{\omega/\gamma}$ position, the theoretical FMR location for $|K_1|/M_0 = 0$. Figure 7 clearly shows that while the initial shifts of the [100] and [111] absorption curves with power are in the proper direction, the limiting field positions of the shoulders have no simple pattern. For [100], the shoulder overshoots $H_{\omega/\gamma}$ by some 30 Oe. For [111], the upsweep profile has both a cusp and shoulder. The latter is not particularly sharp and is located some 20 Oe below $H_{\omega/\gamma}$. For [110] there is little agreement with a heating model. While one would expect the shoulder to appear on the upsweep trace above the low power FMR position, it appears on the downsweep trace about 8 Oe below the low power FMR field. Upsweep yields a cusp close to the low power FMR position. Certain peak and shoulder lineups may also be noted. The relatively sharp shoulders for [100] and [110] occur at the same field, 3365 Oe. The [111] shoulder and [110] cusp occur at about the same field, 3375 Oe. These lineups may be of some significance. Clearly, more is involved here than a simple heating effect which reduces $|K_1|/M_0$.

From Eq. (1) one would infer that there is one orientation, $\theta \cong 29.7°$, where the square bracket term vanishes and the FMR position does not depend on the magnetocrystalline anisotropy. This being the case, one might also infer that for absorption curves in this orientation resonance would occur at $H_{\omega/\gamma}$, indepedent of the incident power level as far as heating effects and the resulting decrease in $|K_1|/M_0$ are concerned. In view of the curious results presented above, this expectation was examined in some detail. The results are shown in Fig. 9. FMR absorption profiles are shown for the $H_{\omega/\gamma}$ orientation angle corresponding to the intersection of the data and the dotted line in Fig. 2 and a zero anisotropy coefficient in Eq. (1), $\sin\theta = 0.8161$. It is clear, especially at the higher powers, that the FMR profile is not independent of power. Shoulders and cusps similar to those discussed above are clearly in evidence.

SUMMARY AND CONCLUSION

Foldover effects seen in the FMR absorption of a single-crystal YIG sphere at moderate power levels consist of resonance curve distortions and shifts in the resonance field, resulting in unusual hysteretic phenomena. These effects are strongly dependent on the crystal orientation with respect to the applied static field, indicating a dependence on the magnetocrystalline anisotropy of the sample.

When experiments are carried out using pulsed microwaves, the observed foldover effects can be seen to be a result of using an overly large duty cycle, or a relatively high average power incident on the sample. This average power dependence of the resonance curve distortions implies sample heating as a cause of the foldover.

The simple heating mechanism outlined in the discussion, involving the reduction of the magnetocrystalline anisotropy by sample heating as resonance is approached, gives a qualitative explanation for the observed effects but is inadequate in several respects. The explanation cannot account for the limiting resonance values falling below $H_{\omega/\gamma}$, the peculiar shapes of the resonance curves seen in some cases, or, most importantly, the resonance shifts that occur when $H_0 = H_{\omega/\gamma}$.

ACKNOWLEDGMENTS

The authors are indebted to Dr. J. J. Green of Raytheon Research Division, Lexington, Massachusetts for providing the YIG sample used in this study, and Dr. Seymour Geller of the University of Colorado, Boulder, Colorado for orienting the sample. The work was supported in part by the United States Army Research Office and the National Science Foundation, Grant DMR-8013727.

[1] M. T. Weiss, Phys. Rev. Lett. **1**, 239 (1958).
[2] M. T. Weiss, J. Appl. Phys. **30**, 2014 (1959).
[3] P. Gottlieb, J. Appl. Phys. **31**, 2059 (1960).
[4] J. I. Masters, J. Appl. Phys. Suppl. **31**, 41s (1960).
[5] J. O. Artman, Phys. Rev. **105**, 62 (1957).
[6] W. H. von Aulock, *Handbook of Microwave Ferrite Materials* (Academic, New York, 1965), p.81.
[7] H. Suhl, Phys. Chem. Solids **1**, 209 (1957).
[8] L. M. Silber, C. E. Patton, and H. F. Naqvi, J. Appl. Phys. **54**, 4071 (1983).

Downloaded 26 Dec 2001 to 129.82.140.114. Redistribution subject to AIP license or copyright, see http://ojps.aip.org/japo/japcr.jsp